Proceedings of the 11th World Congress on Mechanical, Chemical, and Material Engineering (MCM'25)

Paris, France - August, 2025 Paper No. ICMIE 166 DOI: 10.11159/icmie25.166

3D Positioning of a Stewart Platform Using Soft Pneumatic Actuators: A Design Approach

Antonio Šoljić¹, Goran Gregov¹, Ervin Kamenar¹

¹Universtiy of Rijeka, Faculty of Engineering Vukovarska 58, Rijeka, Croatia antonio.soljic@gmail.com; goran.gregov@uniri.hr; ekamenar@uniri.hr

Abstract - In this paper, the application of a novel soft bellows pneumatic actuator (SBPA) into an advanced mechatronic system specifically, a Stewart platform, is investigated. Our previously research has demonstrated that the newly designed SBPA can generate forces exceeding 100 N, achieving a contraction ratio greater than 40% relative to its maximum length, and reaching motion speeds above 60 mm/s. Moreover, precise linear positioning within 10 μm has been achieved through the application of a Linear Quadratic Regulator (LQR). To further evaluate the capabilities of the developed actuator, a six-degree-of-freedom Stewart platform was designed using three identical SBPAs. The 3D positioning of the platform was evaluated under open-loop control, using a camera-based system to track the displacement of key points on the platform for model identification and validation of the control results. The developed Stewart platform achieved a positioning error of 1.1% at the centre of the platform when all SBPAs were activated. Additionally, the platform's dynamic performance was assessed by actuating the SBPA with sinusoidal inputs at varying frequencies. At 1 Hz, the platform exhibited consistent vibrational motion, indicating its potential for use in vibration-based applications. This study advances the development of SBPAs and provides insight into their integration in complex mechatronic systems.

Keywords: soft bellow pneumatic actuator, Stewart platform, position control

1. Introduction

A Stewart platform is a parallel manipulator that provides six degrees of freedom (6-DOF), enabling precise control of motion in three-dimensional (3D) space [1,2]. The manipulator consists of two platforms—one fixed and one movable—connected by either three or six actuators [3,4]. Due to their ability to achieve high precision in positioning, Stewart platforms are widely utilized in various fields, including aerospace, robotics, and medical applications [5,6]. Stewart platforms typically employ pneumatic, hydraulic, or electric actuators [7], coupled with open-loop or closed-loop control systems that utilize advanced control algorithms [8,9].

The advancement of using pneumatic actuators in Stewart platforms lies in their ability to provide high force-to-weight ratios, fast response times, and cost-effective solutions for precise motion control. For example, the study [10] employed six commercial pneumatic cylinders for a developed flight simulator, while the study [11] utilized artificial pneumatic muscles produced by FESTO. On the other hand, new trends in pneumatic and robotics involve the development of soft pneumatic actuators (SPAs) that utilize different design approaches, novel materials, and innovative production technologies [12,13,14]. In our previous study [15], we presented the development of a novel soft bellow pneumatic actuator (SBPA) that utilizes cylindrical bellow geometry and vacuum pressure. The experimental results demonstrate significant performance, with forces exceeding 100 N, contraction ratios over 40%, and maximum velocities above 60 mm/s. Based on the obtained results, the following study [16] was carried out to evaluate the actuators' positioning capabilities using Proportional-Integral-Derivative (PID) and Linear Quadratic Regulator (LQR) controllers. The results indicate that the LQR approach offers superior positioning accuracy, with steady-state errors reduced to a few tens of micrometres, and demonstrates improved dynamic response compared to the PID controller.

This paper presents the design and development process of a Stewart platform with novel soft bellow pneumatic actuators (SBPAs) for actuation. Our contribution advances the performance analysis of the novel SBPA by demonstrating its integration into a real mechatronic system, specifically a Stewart platform. An enhanced version of the SBPA was developed with increased dimensions and additional internal reinforcement rings to better accommodate the specific requirements of the Stewart platform. The designed platform includes a bottom and an upper plate, along with custom-designed connecting

elements for securely attaching the SBPAs to both plates. All components of the platform were fabricated using 3D printing technology. Additionally, a control system was developed by employing predefined voltage signals to proportional pressure regulators, which generate specific vacuum values for each SBPA to produce the desired displacement of the platform. The control system relies on a numerical algorithm developed in LabVIEW to calculate and coordinate the actuation of each SBPA, enabling the intended 3D positioning of the Stewart platform's upper plate. The design approach used in this research is summarized in Figure 1.

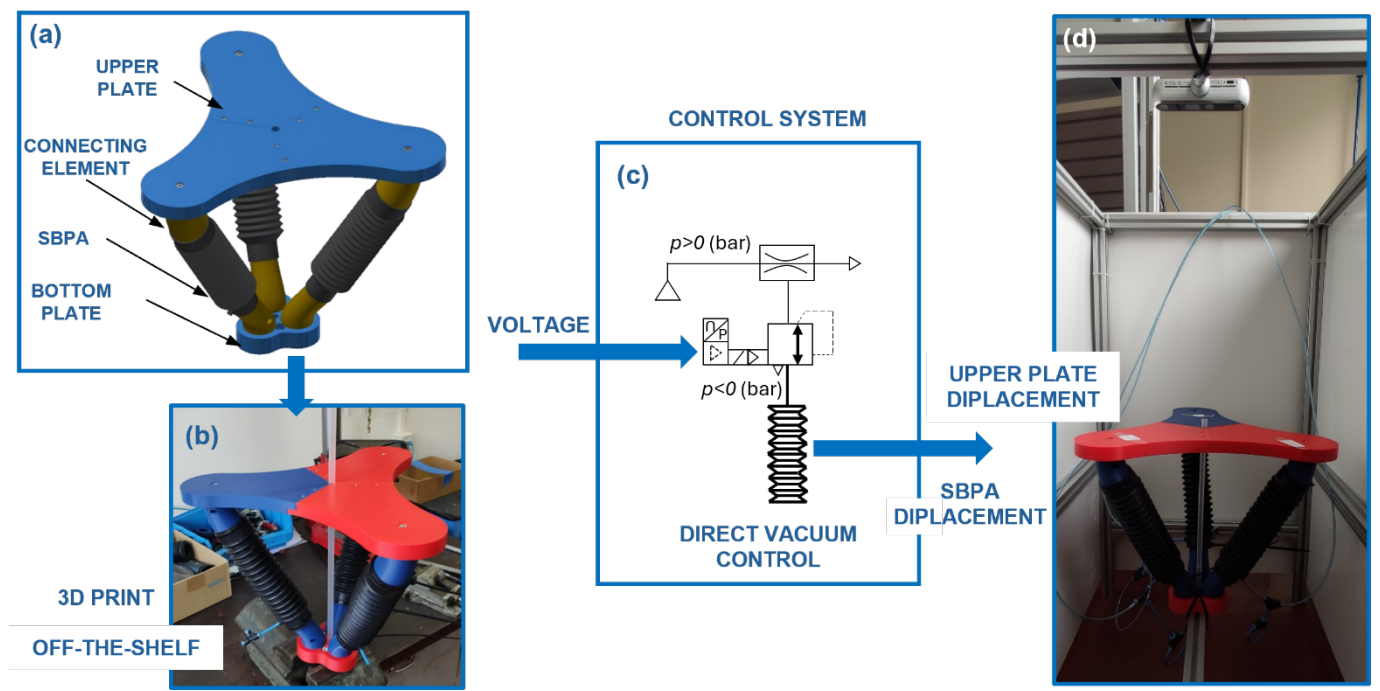


Fig. 1: a) 3D model of the Stewart platform with its main elements, b) manufactured and assembled Stewart platform, c) schematic view of the control system, d) Stewart platform mounted and tested on the test-bench

The remainder of the paper is organized as follows: Section 2 describes the materials and methods, including the design and fabrication of the Stewart platform utilizing a soft bellow pneumatic actuator, the experimental apparatus, and the development of the control system. Section 3 presents the results and discussion. Finally, Section 4 summarizes the main conclusions.

2. Materials and methods

In this section, a brief introduction to the design and fabrication of the Stewart platform with soft bellows pneumatic actuators is provided. Additionally, the complete experimental setup and its key components are presented, including the development of the control system.

2.1. Design and Fabrication of Stewart Platform Utilizing Soft Bellow Pneumatic Actuators

The design of the Stewart platform is based on a comprehensive analysis of existing configurations, as well as the application of newly developed SBPA. Drawing from previous research [15,16], an enhanced version of the SBPA was created with increased dimensions to achieved specific requirements of the Stewart platform. The upgraded SBPA has a total length of 200 mm and a contraction capability of 120 mm, corresponding to a maximum contraction ratio of 40%. The bellows feature an outer diameter of 61.5 mm and a wall thickness of 2 mm. A key structural improvement in the revised SBPA is the placement of reinforcement rings in every fold of the bellows, unlike the earlier design which included rings in

every second fold. This modification enhances the actuator's load-bearing capacity, though it slightly reduces the overall contraction range. However, the increased size of the bellows compensates for this reduction, ensuring that the Stewart platform's functionality remains unaffected.

The Stewart platform was designed with SBPAs positioned between the bottom and upper plates at a 60° inclination, arranged in a circular pattern with uniform 120° spacing, as shown in Figure 1a. This arrangement provides sufficient space for the connecting elements between the SBPAs and the bottom plate. Both plates are 25 mm in height, with the upper plate having a diameter of 400 mm and the bottom plate measuring 100 mm in diameter, ensuring structural reliability. The connection between the connecting elements and the SBPAs is secured through a tight fit and tension tie, while screw joints are used to fasten the elements to both the bottom and upper plates. All components of the platform were manufactured using 3D printing technology with PLA material.

To ensure accurate positioning of the upper plate relative to the bottom plate in a neutral position, without interfering with the platform's movement during operation, a combination of elasticity and rigidity was required. To meet this need, a needle spring solution was implemented, utilizing a 10 mm diameter PVC pipe with a 1 mm wall thickness. The needle spring is centrally located on the bottom plate and secured with an adhesive joint. The needle spring serves multiple functions: it facilitates smooth Z-axis movement of the upper plate and acts as a return spring, ensuring the upper plate returns to its initial position once the SBPA actuation is complete. The complete assembly of the Stewart platform, including the added needle spring, is shown in Figure 1b. After assembly, a series of tests were conducted to assess the platform's operational performance, including measuring the maximum displacement of each SBPA to evaluate its operational workspace. The results confirm that the platform successfully achieved the required range of motion necessary for its intended functionality.

2.2. Experimental Apparatus

The experiments were carried out at the Hydraulic and Pneumatic Laboratory at the University of Rijeka, Faculty of Engineering. The pneumatic apparatus consists of a Ceccato CSM 7.5 D compressor, a FESTO LR-MICRO-MA40-Q4 manual pressure regulator, a FESTO VN-05-H-T2-PQ1-VQ1-RQ vacuum generator, FESTO VPPI-5L-G18-1V1H-V1-S1D, and Enfield TR-010-v-ex proportional pressure regulators. The measuring equipment used for control and data acquisition includes the National Instruments NI myRIO 1900 device, Schmalz VS VP8 SA M8-4 vacuum and pressure sensors, and Intel RealSense Depth Camera D455.

The main task of the pneumatic apparatus is to generate a vacuum utilized for actuating SBPAs. The vacuum is achieved by a FESTO vacuum generator operating on the Venturi principle, converting an input pressure range of 0 to 4.5 bar into a vacuum range of 0 to -0.88 bar. Consequently, the input pressure was manually regulated using a pressure regulator to achieve the maximum value of p=4.5 bar. The displacement of the SBPA depends on the vacuum value, which is controlled by proportional pressure regulators. Each of the three SBPAs is assigned an individual proportional pressure regulator to manage its respective vacuum value. One FESTO VPPI proportional pressure regulator and two Enfield TR proportional pressure regulators are used for this purpose. The applied solution for vacuum control represents a direct vacuum control approach (Figure 1c), which has shown a faster response time of the SBPA in our prior research [16]. The Enfield TR proportional pressure regulator does not possess an internal pressure sensor like the FESTO VPPI pressure regulator. Instead, it relies on an external pressure sensor, and in this case, a Schmalz sensor is used to provide feedback for controlling the output pressure. To adjust the parameters of the control system, software provided by the manufacturer is utilized, enabling the definition of pressure limit values and the adjustment of PID parameters. According to the manufacturer's recommendations, the advised PID parameters are P=40%, I=20%, D=10%. Additionally, a calibration procedure was conducted for both Enfield TR pressure regulators to fine-tune their response to the input pressure value.

To verify the accuracy of the 3D displacement measurements of the platform's upper plate, a laboratory test bench was constructed using standard strut profiles, designed to securely mount the Stewart platform and ensure precise positioning relative to the camera, as shown at Figure 1d. The camera, equipped with dual depth sensors, an RGB sensor with a global shutter, an infrared projector, and an integrated IMU, was used to enable precise 6-DOF measurements with enhanced accuracy. It is also supported by software that enables real-time visualization of depth sensor images, 3D points cloud rendering, as well as recording and playback capabilities. The camera settings were adjusted to optimize measurement results,

with a maximum depth of field set to 2.5 m. Considering that the upper platform is positioned 0.4 meters from the camera, this configuration achieved a nominal precision of up to 1 mm.

2.3. Development of Control System for a Stewart Platform

The control system operates by using a predefined input signal to achieve the desired output, relying solely on the system's inherent dynamics without feedback or adjustments based on the actual response. To control the 3D position of the Stewart platform's upper plate, the input values correspond to the vacuum values of each individual SBPA, along with the voltage values supplied to the proportional pressure regulators. The primary objective of the open-loop control system is to develop an algorithm that coordinates the three-dimensional positioning of the upper platform. The software algorithm identifies which SBPAs require actuation and calculates the necessary vacuum/voltage values for each proportional pressure regulator to induce the required displacement. This control software, developed using LabVIEW, ensures seamless communication with the NI myRIO 1900 control hardware.

To maintain the upper platform in a neutral position and enable its load-holding capability, it is necessary to apply a positive pressure slightly above atmospheric pressure. Experimental testing was conducted to determine the maximum positive pressure value for each SBPA and its corresponding proportional pressure regulator, with the goal of precisely identifying the maximum voltage value for the desired pressure value. The determined maximum voltage values are as follows: 5.1 V for the FESTO proportional pressure regulator (it will be referred to as label A), 0.78 V for the first Enfield proportional pressure regulator (label B), and 0.58 V for the second Enfield proportional pressure regulator (label C). Differences in voltage values arise from the use of different pressure regulators, while variations between identical B and C pressure regulators can be attributed to the use of different calibrated external pressure sensors.

The development of the control algorithm requires system identification, which involves experimental measuring platform displacements relative to the voltage values of the proportional pressure regulators. Specifically, displacements of predefined points A, B, and C, representing the connection points of the SBPAs and the platform, are quantified. For each specific voltage value (U), all three spatial coordinates of each point are measured. Subsequently, based on these values, the spatial distance (diagonal) between the coordinates of the points is computed, representing the displacement (D) of the SBPA. The coordinate system's origin is set at the centre of the upper platform. Measurements are conducted up to the maximum displacements of all SBPAs, delineating the platform's maximum workspace. SBPA displacement (D) is calculated using equation (1) to determine the distance between the measured displacement point (A_1 , B_1 , C_1) and the initial point (A_0 , B_0 , C_0) in 3D space, where x, y, and z represent the spatial coordinates of each point.

$$D(A_1, B_1 C_1; A_0, B_0, C_0) = \sqrt{(x_1 - x_0)^2 + (y_1 - y_0)^2 + (z_1 - z_0)^2}$$
(1)

TO 1.1 1 TO CODD 1 11 1	(TD) 0 11:00 1:	(TD 1	
Table 1: The SBPAs displacem	ient (/)) for different voltage	e (U) and vacuum pressure (n) values

	SBPA A			SBPA B			SBPA C	
<i>U</i> , V	p , bar	D , mm	U, V	p , bar	D , mm	U, V	p , bar	D , mm
0.2	-0.04	37.9	0.04	-0.05	23.5	0.04	-0.07	23.2
0.4	-0.08	102.3	0.08	-0.1	26.6	0.08	-0.14	49.4
0.6	-0.12	115.2	0.12	-0.15	46.5	0.12	-0.21	76.8
0.8	-0.16	116	0.16	-0.2	68.8	0.16	-0.28	98.6
1	-0.2	117.1	0.20	-0.25	85.9	0.20	-0.35	112.2
1.2	-0.24	119	0.24	-0.3	93.6	0.24	-0.41	122.8
			0.28	-0.35	100.8	0.28	-0.48	129.8
			0.32	-0.41	108.6	0.32	-0.55	131.9
			0.36	-0.46	108.6	0.36	-0.62	132.7

Based on the mentioned, displacement values for the utilized SBPAs were attained for specific voltage/vacuum values of the proportional pressure regulators, as outlined in Table 1. Differences in the obtained displacement values corresponding

to specific voltage and vacuum values can be observed. These differences stem from variations in the operational conditions of the SBPAs, notably differences in the initial vacuum values associated with different proportional pressure regulators, as well as differences among individual Enfield TR pressure regulators, as previously explained. Based on experimentally measured values of voltage (U) and displacement (D) for each SBPA, a third-order polynomial curve was derived (equation 2) and integrated into the control algorithm. The polynomial coefficients (a, b, c, d) for each SBPA are provided in Table 2.

$$U(D) = a \cdot D^3 + b \cdot D^2 + c \cdot D + d \tag{2}$$

Table 2: Regression polynomial coefficients.

	а	b	с	d
SBPA A	5.10-6	-9.97·10 ⁻⁴	6.5027 · 10-2	-1.1
SBPA B	4.10-7	-4.93·10 ⁻⁵	3.7068 · 10-3	0
SBPA C	5.10-7	-1.002 · 10-4	7.1239·10 ⁻³	-8.10255 · 10-2

Furthermore, the control algorithm has been enhanced to enable the actuation of the SBPAs through the utilization of a sinusoidal signal generated by a subroutine capable of producing diverse waveform signals. This functionality empowers the platform to execute oscillatory motion, a feature of significant interest particularly in scenarios where the platform serves as a vibration device for laboratory testing purposes. The sinusoidal signal encompasses several key parameters, including amplitude, frequency, phase shift, and mean value displacement. These sinusoidal signals are directly interfaced with the signal transmission module of the proportional pressure regulators, circumventing the 3D platform position control algorithm.

3. Results and discussion

After developing and validating the control system, experimental measurements were conducted to assess the achievable 3D positioning and precision of the Stewart platform. Figure 2 illustrates the results of the maximum displacement, showing the displacement ranges for characteristic points on the upper plate. The graphical representation was created by adding the achieved displacement value to the initial distance of each measured point from the centre of the platform. These displacements were measured both when only one SBPA (A, B, or C) was actuated and when combinations of two pairs of SBPAs (AB, BC, or AC) were activated. It is noteworthy that the attained displacements of each SBPA are significantly smaller compared to the linear displacement of an individual SBPA. This happening can be attributed to the design of the platform and the inherent limitations when multiple SBPAs are actuated simultaneously. Specifically, the maximum displacement for point A is 119 mm, for point B is 108.5 mm, and for point C is 132.7 mm. Additionally, the maximum displacement for point AB is 87.7 mm, for point BC is 104.4 mm, and for point AC is 99.2 mm.

A comparative analysis was conducted to validate the precision of the developed open-loop control system in achieving the 3D positioning of the Stewart platform's upper plate. This analysis compared the desired position values of the platform with the position values measured by the camera. The 3D position of the platform is determined by the displacement required for each SBPA to reach the desired platform position. Multiple iterations were performed, and measurements were recorded for the positions of characteristic points (A, B, and C) on the upper platform as well as the centre of the platform and the obtained results are presented in Table 3. It is evident from the results that the positioning error ranges between 1.3% and 9.4%. These error values are considered highly satisfactory, particularly when considering the precision of the camera used, which boasts a measurement accuracy of only 1 mm. Notably, larger deviations are evident when positioning the outer points of the platform, namely A, B, and C. This occurrence can be attributed to the non-activation of all SBPAs in these instances. However, when positioning the centre of the platform with all SBPAs activated, the error diminishes substantially, reaching an error of 1.1%.

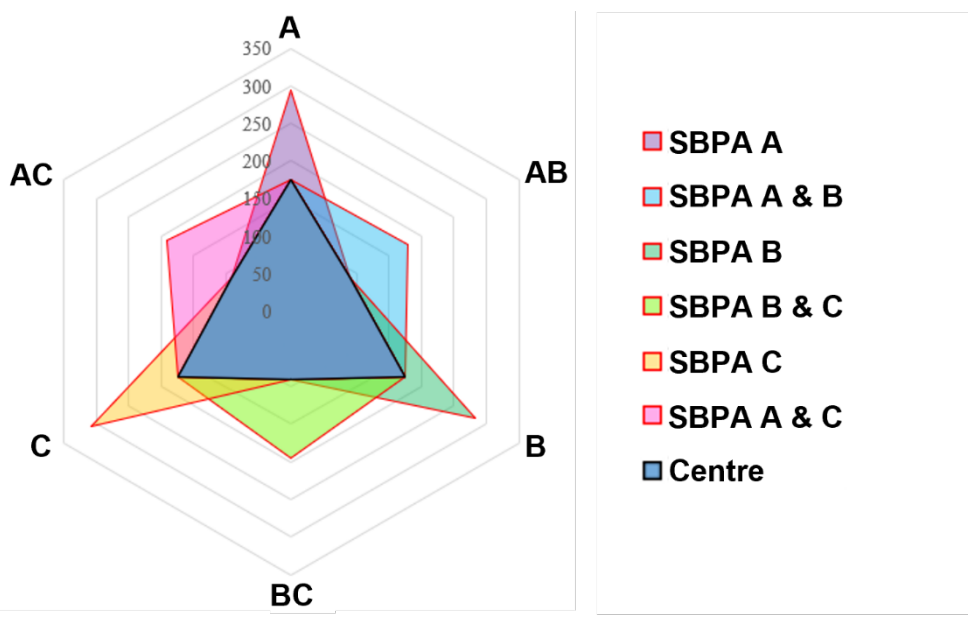


Fig. 2: The maximum displacement of each individual SBPA and their combination.

Measurements were also conducted to observe the motion when the SBPAs were actuated with sinusoidal signals of varying frequencies. For the analysis, low frequencies of 0.01 Hz and a higher frequency of 1 Hz were selected. A frequency of 0.01 Hz was deemed optimal for demonstrating and examining the long wave-like motion of the platform, with each SBPA achieving displacements of up to 50 mm. Conversely, a higher frequency of 1 Hz facilitated a standard vibrational motion of the upper platform, making it suitable for application as a vibration device. However, it is essential to note that the vibration characteristics were not the primary focus of this study, as the analysis at higher frequencies was not considered. The incorporation of oscillatory motion aimed to illustrate additional possibilities for further research and applications of the platform.

Table 3: Comparison of referent and output displacements

	Referent D _{ref} , mm	Output D, mm	Error, %
SBPA A	30	31.4	4.7
	80	74.1	7.4
SBPA B	40	37.3	6.6
	80	77.6	3.0
SBPA C	40	41.2	2.9
	80	76.9	3.9
SBPA A&B	30	28.3	5.7
	80	72.4	9.4
SBPA B&C	30	27.8	7.3
	55	51.8	5.9
SBPA A&C	30	27.7	7.6
	55	52.3	5.0
Centre	40	39.0	2.5
	80	79.0	1.3

4. Conclusion

Based on previous research [15,16] into the newly developed soft bellows pneumatic actuator (SBPA) and its good performance characteristics, further investigation was carried out by integrating the actuator into a complex mechatronic system. The Stewart platform, a well-known parallel manipulator, was selected for this purpose due to its ability to provide six degrees of freedom through a configuration of two parallel plates connected by at least three actuators. The inherent complexity of the Stewart platform calls for a sophisticated control system capable of ensuring precise positioning of the upper plate in 3D space. To facilitate this study, a custom Stewart platform was designed and fabricated using 3D printing technology. The platform was equipped with three upgraded SBPAs, which were scaled up from the original design to meet the system's mechanical and spatial requirements. Each SBPA is independently controlled by a dedicated proportional pressure regulator. An open-loop control system was implemented to drive the SBPA, with camera-based monitoring employed to track the displacement of the upper platform and evaluate its operational workspace.

The experimental results clearly demonstrate the effectiveness of the Stewart platform's workspace when actuated by individual SBPAs or their combinations. Maximum displacements were precisely measured for each actuator: 119 mm for SBPA A, 108.5 mm for SBPA B, and 132.7 mm for SBPA C. Validation of the open-loop control system produced satisfactory 3D positioning of the upper platform plate, with positioning errors ranging from 1.1% to 9.4%. Higher deviations were observed when targeting points near the platform's boundary, which can be attributed to factors such as mechanical tolerances, performance variations among SBPAs, and the system's inherent dynamic behaviour. In contrast, positioning the centre of the platform using all SBPAs resulted in a significantly reduced error of just 1.1%. Additionally, dynamic performance tests were conducted by actuating the SBPAs with sinusoidal signals at various frequencies. Frequencies of 0.01 Hz and 1 Hz were found to produce the most stable and consistent motion. Notably, actuation at 1 Hz induced smooth vibrational motion of the upper platform, indicating the system's potential application as a vibration-generating device.

Future research will primarily focus on overcoming the challenges associated with position control of the Stewart platform through a closed-loop approach. This will likely involve refining the algorithms used in accelerometer and gyroscope modules, as well as integrating advanced filtering techniques—such as Kalman filtering—commonly employed in comparable systems to improve signal accuracy and stability. Additionally, the development of camera-based object tracking algorithms will be pursued to further enhance the precision and reliability of the platform's position control.

Acknowledgements

The research was funded by the University of Rijeka Grants: *Development and Design of Soft Pneumatic Actuators for Multi-Axis Motion Systems* (uniri-iskusni-tehnic-23-174) and *Rehabilitation devices based on soft robotics and biomechatronic sensors* (uniri-iskusni-tehnic-23-47).

References

- [1] D. Stewert, (1966). A platform with 6 degrees of freedom. In *Proc. IMech E* (Vol. 180, pp. 371-386).
- [2] B. Dasgupta and T. Mruthyunjaya, (2000). The Stewart platform manipulator: a review. Mechanism and machine theory, 35(1), 15-40.
- [3] M. Furqan, M. Suhaib, and N. Ahmad, (2017). Studies on Stewart platform manipulator: A review. Journal of Mechanical Science and Technology, 31, 4459-4470.
- [4] Q. Gu, J. Tian, B. Yang, M. Liu, B. Gu, Z. Yin, ... and W. Zheng, (2023). A novel architecture of a six degrees of freedom parallel platform. Electronics, 12(8), 1774.
- [5] M. Wapler, V. Urban, T. Weisener, J. Stallkamp, M. Dürr, and A. Hiller, (2003). A Stewart platform for precision surgery. *Transactions of the Institute of Measurement and Control*, 25(4), 329-334.
- [6] L. Herrera, S.B. Lin, S.J. Montgomery-Smith, and Z.O. Williams, (2024, August). Modeling of a Stewart Platform for Analyzing One Directional Dynamics for Spacecraft Docking Operations. In *International Conference on Physical Systems Modeling, Simulation Models and Dynamic Models*.
- [7] X. Yuan, Y. Tang, W. Wang, and L. Zhang, (2021). Parametric Vibration Analysis of a Six-Degree-of-Freedom Electro-Hydraulic Stewart Platform. *Shock and Vibration*, 2021(1).

- [8] H. Tourajizadeh, M. Yousefzadeh, and A. Tajik, (2016). Closed loop optimal control of a stewart platform using an optimal feedback linearization method. *International Journal of Advanced Robotic Systems*, 13(3), 134.
- [9] D. Li, S. Wang, X. Song, Z. Zheng, W. Tao, and J. Che, (2024). A BP-Neural-Network-Based PID Control Algorithm of Shipborne Stewart Platform for Wave Compensation. *Journal of Marine Science and Engineering*, 12(12), 2160.
- [10] J. Pradipta, M. Klünder, M. Weickgenannt, and O. Sawodny, (2013, July). Development of a pneumatically driven flight simulator Stewart platform using motion and force control. In 2013 IEEE/ASME International Conference on Advanced Intelligent Mechatronics (pp. 158-163). IEEE.
- [11] V. Volkov, A. Polyakov, and Y. Chepenyuk, (2011). Structure and kinematics of the stand for testing implants with actuator on the basis artificial pneumatic muscle. *Journal of Biomechanics*, 44, 20.
- [12] Y. Jung, K. Kwon, J. Lee, and S.H. Ko, (2024). Untethered soft actuators for soft standalone robotics. *Nature Communications*, 15(1), 3510.
- [13] G. Gregov, T. Vuković, L. Gašparić, and M. Pongrac, (2025). Development, Experimental Assessment, and Application of a Vacuum-Driven Soft Bending Actuator. *Applied Sciences*, 15(5), 2557.
- [14] S. Joe, M. Totaro, H. Wang, and L. Beccai, (2021). Development of the ultralight hybrid pneumatic artificial muscle: Modelling and optimization. *PloS one*, *16*(4).
- [15] G. Gregov, T. Ploh, and E. Kamenar, (2022). Design, development and experimental assessment of a cost-effective bellow pneumatic actuator. In *Actuators* (Vol. 11, No. 6, p. 170).
- [16] G. Gregov, S. Pincin, A. Šoljić, and E. Kamenar, (2023). Position Control of a Cost-Effective Bellow Pneumatic Actuator Using an LQR Approach. In *Actuators* (Vol. 12, No. 2, p. 73).